Annals of Nuclear Energy 212 (2025) 111061

Contents lists available at ScienceDirect

Annals of Nuclear Energy

journal homepage: www.elsevier.com/locate/anucene

Investigation of nuclide inventory of cladding material irradiated in the Goesgen PWR core

R. Dagan [a,*], T. König [a], M. Herm [a], F. Alvarez [b], E. Dorval [d], S. Häkkinen [d], E. Vlassopoulos [c], A. Shama [c], A. Smaizys [e], P. Schillebeeckx [f]

[a] Institute for Nuclear Waste Disposal (INE), Karlsruhe Institute for Technology (KIT), Karlsruhe, Germany
[b] Centro de Investigaciones Energéticas, Medioambientales y Tecnológicas, CIEMAT, Madrid, Spain,
[c] National Cooperative for the Disposal of Radioactive Waste (Nagra), Wettingen, Switzerland
[d] VTT Technical Research Centre of Finland, Finland
[e] Lithuanian energy Institute (LTI), Nuclear Engineering Laboratory, Kaunas, Lithuania
[f] European Commission, Joint Research Centre (JRC), Geel, Belgium

A B S T R A C T

A characterization of the spent nuclear fuel (SNF) for its radionuclide (RN) inventory is vital for various back-end stages of the nuclear fuel cycle. It concerns both the fuel and the metallic (i.e., cladding and structural material) components of the spent fuel assemblies, where different calculation approaches and methods should be deployed for their characterization. This study concentrates on fuel traces and other impurities within the cladding. During the operating cycles, the Zircaloy cladding is exposed to a considerable amount of irradiation. The impact of the exposure should be checked to assure the integrity of the cladding and thus the safety of the stored spent fuel. Within the work package "Spent Nuclear Fuel Characterization and Evolution until Disposal" (SFC) of the EURAD project, dedicated samples were produced, irradiated and the radionuclide inventory of the cladding was analysed and compared. In parallel a blind test was performed, in which different partners used different codes to simulate the irradiation quantity. The blind test showed good agreement between most of the codes, in particular in view of the small amount of the evolved fuel traces. Furthermore, the presence of actinides, caused by precipitation of uranium on the inner surface of the cladding during manufacturing, was found to be negligible in comparison to precipitation of traces of fuel pellets on the cladding during operation. The good agreement between the simulating codes enables to depict further the initial amount of alloying elements of the cladding material itself in a better manner. In particular specific isotopes of cobalt, nickel and iron, which are directly connected to the unique properties of each cladding material can be better identified based on the accurate measuring techniques used in this study.

1. Introduction

The licensing, construction and commissioning of a final repository site for high-level waste, forces several countries to store their irradiated fuel assemblies either in spent fuel pools or in dual-purpose casks in dry interim storage facilities. For the latter conditioning of the fuel assemblies for final disposal, cladding integrity of the irradiated fuel rods is of utter importance. However, due to the in-pile conditions, transuranic elements come in contact with the cladding, which could cause defects through energetic alpha emittance, that, in addition to hydrogen embrittlement, impact the integrity of the cladding during interim storage considerably. Furthermore, heat is generated in large amounts due to decay of radioactive nuclides within the rods. The decay heat and the radiation type are of high importance for disposal licensing procedures.

Therefore, a proper characterization, by using neutronic calculation and burn-up codes, of spent nuclear fuel (SNF) assemblies is required for operational and long-term safety assessments including prolonged dry interim storage and final disposal. Many studies focus on identifying the radionuclide inventory of SNF assemblies, as summarised by e.g., Sjöland et al.,(Sjöland et al, 2023) Zerovnik et al.(-Žerovnik, G., Ambrožič, K., Čalič, D., Fiorito, L., Govers, K., Hernandez Solis, A., Kos, B., Kromar, M., Schillebeeckx, P., Stankovskiy, A.: Characterisation of spent PWR fuel for decay heat, neutron and gamma-ray emission rate: code comparison,' Proceedings of the International Conference on Mathematics and Computational Methods applied to Nuclear Science and Engineering (MC, 2019). or Rochmann et al. (Dimitri Alexandre Rochman, 2023) where available radiochemical analysis-based measurements (of the OECD NEA database (SFCOMPO2.0) (Michel-sendis et al., 2017) were compared successfully with different burn up codes. However, radiochemical analyses of irradiated nuclear fuel rod claddings are scarce. Moreover, the extensive research towards new cladding types the so called ATF (Accident tolerated fuels) cladding materials (Steinbrueck et al., 2024; Kim et al., 2022; Alraisi et al., 2022; Doyle

* Corresponding author.

https://doi.org/10.1016/j.anucene.2024.111061
Received 31 July 2024; Received in revised form 6 November 2024; Accepted 11 November 2024
Available online 22 November 2024

et al., 2023; Qiu et al., 2020), increases the need for reliable cladding benchmarking, which eventually should help to avoid efficiently accidents like the one in Fukushima. In particular, by developing new methods for cladding radiochemical analysis parallel to improved burnup codes, one could assess adequately a specific material composition under investigation. In view of the fact that for the new ATF, FeCrAl alloys are to be used, which are not in general fission products, one can estimate their activation products and calculate backwards the original concentration of a certain isotope of the precursor nuclide. Hence, the following study serves, among others, as a preliminary step towards the future employment of ATF cladding materials. The goal of this study is to depict the nuclide vector of the cladding of spent nuclear fuel of a pressurized water reactor, for which a dedicated sample was prepared and irradiated. The advantage of the current study lies in the ability of using the state-of-the-art measurement techniques in the KIT –INE hot cell facility, and to compare the experimental data with results of different codes using different neutron transport and burn up modules. In particular, diverse stochastic and deterministic codes were introduced.

In the next sections, the two-step benchmark between the codes will be presented. The first step is the blind test phase and the second the correction phase and the discussion for the source of deviations. A comparison between calculated and experimental data is presented at the end. It leads to a practical safety analysis concerning the high quality of the manufacturing techniques of the samples (Hakkinen, 2024) and fuel rods in general, in which the integrity of the cladding of spent fuel in storage facilities is only affected by the operation conditions.

2. Code-to-Code benchmark

The calculation of the radionuclide inventory within the cladding is by far more sensitive to the calculation methods as for the calculation of fuel pellets. Within the cladding, one expects only traces of uranium during manufacturing, as was assessed by (Hakkinen, 2024). Strictly speaking, the concentration of uranium impurities within the cladding is seven orders of magnitude smaller than within the fuel pellets. This fact imposes obviously a corresponding challenge on the numerical solvers, in particular those that deal with stochastic methodologies due to the need of sufficient statistics for specific reactions.

The codes used for the benchmark were MCNP and its burn up code module CINDER (Gallmeier et al., 2010) with ENDFB-VII library, the Serpent code and its own burn up solver (Leppänen, 2015; Pusa and Leppänen, 2010) with JEFF version 3.1.2, MCNP with the EVOLCODE burn up option (Alvarez-Velarde et al., 2014)and JEFF library 3.3.The Polaris (B.J. Ade. SCALE/TRITON Primer: A Primer for Light Water Reactor Lattice Physics Calculations. Tech. rep. ORNL/TM-, 2012) and TRITON (A. Shama et al. "Validation of spent nuclear fuel decay heat calculations using Polaris, ORIGEN and CASMO5". In: Annals of Nuclear Energy 165, et al., 2022) modules of the SCALE Code System using the ORIGEN (ORIGEN2.2 ORNL, USA, CCC-371, 2002) burn up module. For those codes the ENDFB-VII in its group structure form was employed.

Different users participated in the benchmark in a blind test manner using the same irradiation conditions of a fuel segment that was irradiated in the Goesgen reactor in Switzerland (Stratton et al., 1991). The results refer to the so-called plenum area in which the cladding surrounds a stainless-steel spring on the top of the pellets as shown in the schematic configuration in Fig. 1. The irradiation conditions included 4 cycles of total 1226 irradiation days reaching an averaged burn up of 50.4 MWd/kg. The segment was discharged on 17.05.1989 and the cooling time was adjusted to the measurement day, i.e. 1.12.2020.

The output was the specific activity of several isotopes, expressed in Bq/g. Fig. 2 shows results of the blind test phase concerning curium and

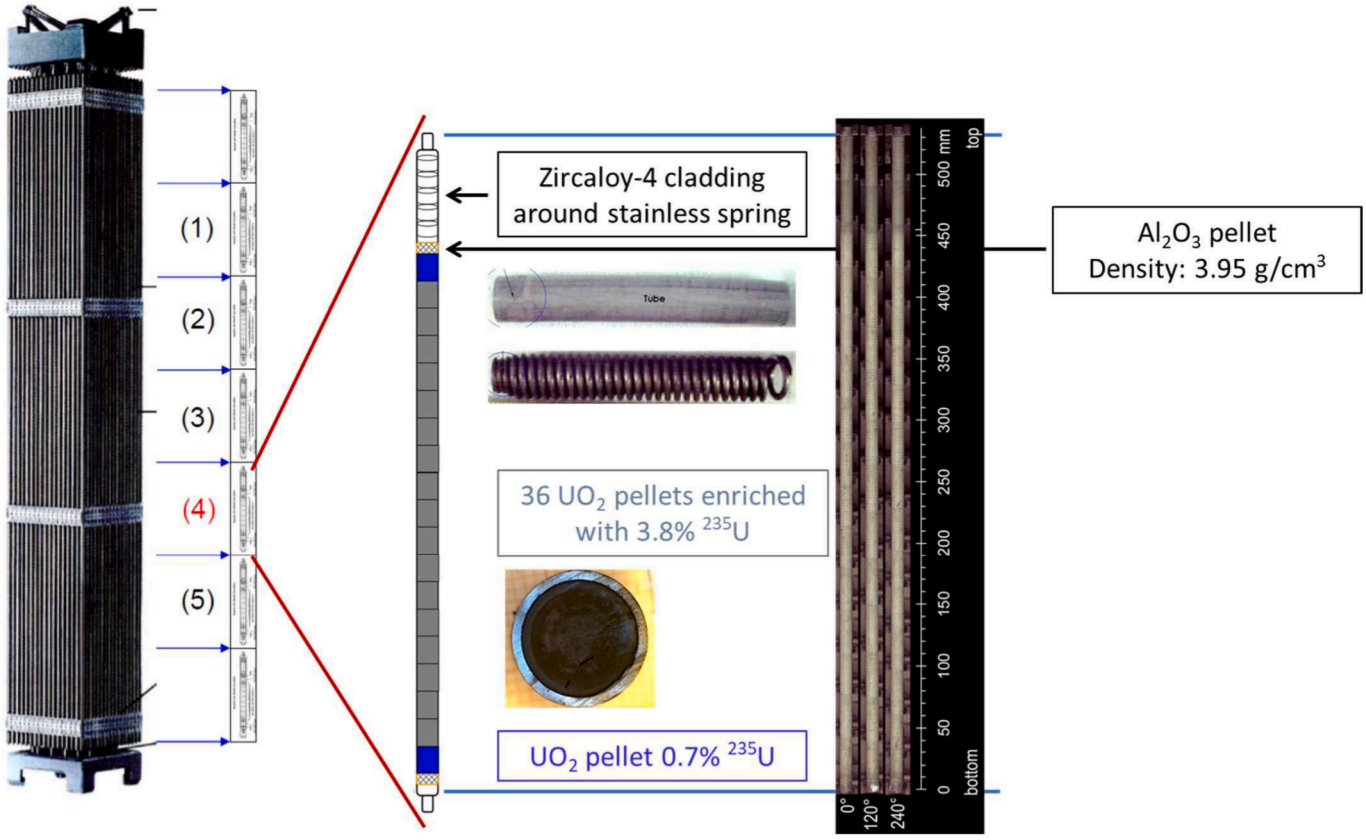

Fig. 1. Schematic configuration of the benchmark. The segment located at position 4 in one of the rods of a 15X15 subassembly. The upper part of the probe contains cladding around the stainless-steel spring. Figure modified from (B. Kienzler, V. Metz, L. Duro, A. Valls, 1st Annual Workshop Proceedings of the Collaborative Project "Fast/Instant Release of Safety Relevant Radionuclides from Spent Nuclear Fuel"(7th EC FP CP FIRST-Nuclides), 2014).

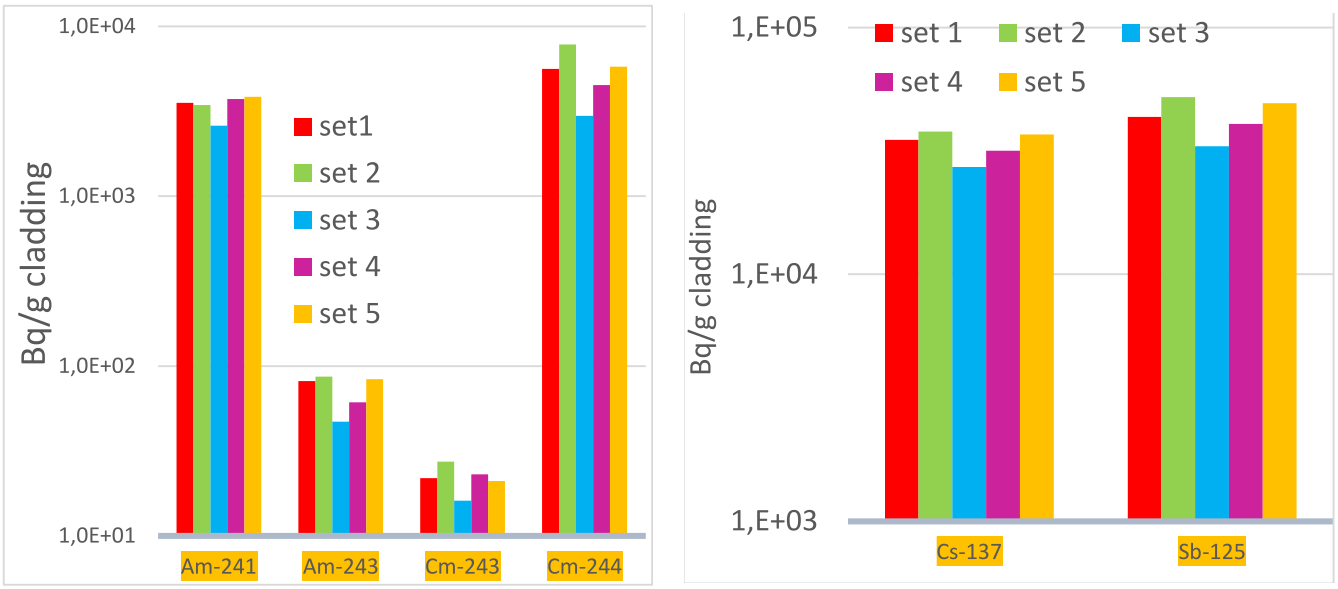

Fig. 2. A. log based blind test simulation results for am-243 and cm-244 isotopes from the plenum of the goesgen sample. b. log based blind test simulation results for cs-137 and sb-125 from the plenum of the goesgen sample.

americium isotopes (2a), Cs-137 and Sb-125(2b) respectively. This figure illustrates the largest differences, as one would expect, in the inventory of Cm-244 using different codes. Differences of AM243, which is in the build-up chain of Cm244, are of the same shape but to some extent smaller. The differences between codes for Cs-137 (representing the fission process) and Sb125 (mainly coming from Sn-124) show again a similar shape to the actinides. Those results point out that there were no preliminary errors concerning the input data and other ambiguities within the definition of the benchmark. In such cases one would not expect a consistence shape of the results. Further, the differences show an overall acceptable agreement as far as nuclear data and different codes and methodologies are concerned. Nevertheless, the need for accurate results lead to an extensive analysis concerning the flux and/or geometry distribution or specific burn up module methodologies which are discussed in the next section

In Figs. 3 and 4 results for other nuclides are presented. Fig. 3 shows the results for the uranium and plutonium vector in the cladding at the plenum. Fig. 4 emphasizes the discrepancies of the most important radionuclides contributing to the dose using a linear scale. The most extreme case is the difference between the maximum and minimum inventory value of Cm-244 which amounts to 58 %. For other nuclides, the differences between the 5 different codes are by far lower. Consequently, the agreement is in general good considering the small amount of traces and the uncertainties expected due to nuclear data, in particular Cm-244, as will be discussed in the next section.

3. Analysis of the simulated nuclide inventory

A detailed analysis of differences between results of different codes is performed in a conservative form. Strictly speaking, the maximum

Fig. 3. Log-based simulation results for the uranium and plutonium vector of the benchmark.

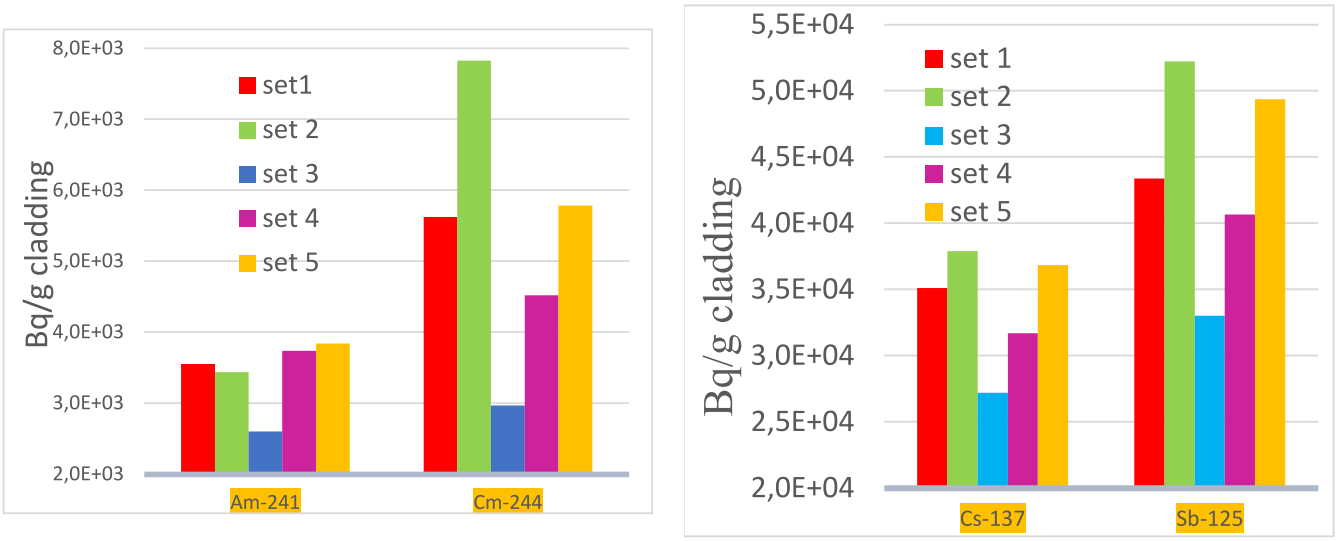

Fig. 4. A. linear based comparison for am-241 and cm-244 isotopes of the goesgen sample. b. linear based comparison for cs-137 and sb-125 isotopes of the goesgen sample.

difference between results of the 5 codes is discussed without looking at average results as each of the codes and calculation methods are legitimate, and therefore, each of those results should be dealt with, in an equal manner.

In particular, Table 1 reports the calculated values obtained with the different codes for Cm-244 and Cs-137. For Cm-244 the results of set 2 are by far higher so there might be a specific issue in one or more of the codes. However, for Cs-137, there is no code which introduces extremely low or high results. Cs-137 is an indicator for the quality of fission and hence flux distribution. Thereafter for the blind test phase all data are expectable in a sense that no extreme user error on the input data can be identified and the differences come indeed from the performance of the calculation tools.

The fact that the calculations deal with traces of uranium, seven order of magnitude smaller than the density of the fuel itself can cause minor discrepancies (few percent) which are for the investigation of the cladding of negligible importance. More important is the diversity of the codes involved in the current study. Out of the five codes, two are deterministic and the stochastic codes are divided into two different solver approaches used in MCNP and Serpent. Further, the depletion codes used in connection with the above flux simulators are divided into formally 4 types of the Bateman equation solution procedure, some of which depend strongly on the chosen decay process, namely the periods for which the nuclide inventory is kept constant.

From Fig. 3 it can be seen that all the above arguments are all of the same order of magnitude, at quite low values. The relative deviations sum up to about 25–30 % between the minimal and maximal values of the compared simulations. Fig. 4a deals with americium and curium where bigger differences are expected. Indeed, for Cm-244 the maximal deviation between the codes is as discussed above 50 %. This value is obtained between the data set 2, which showed higher values for almost all nuclides and data set 3, which showed stronger tendency for lower values. One explanation for the differences can be deduced from Fig. 4b. The differences between the codes and the solvers techniques can be usually detected by Cs-137 and Nd-148. The maximal differences for the calculated Cs-137 inventory is about 25 %. A similar difference (~25 %) was also obtained for the calculated Nd-148 concentration. Thereafter, all other comparisons of the burned up nuclides show differences up to about 30 %, namely as expected in accordance with the Cs-137 and Nd-148 results. Nevertheless, it is evident that the results should be further improved, in particular for low concentration of fuel, at least to the level of the nuclear data uncertainties discussed below.

In view of the comparison with experimental results and in accordance with the deviations between the codes as discussed above, the uncertainties of the nuclear data themselves were analysed, using the well-known experimental benchmark of the Takahama-3 reactor (OECD NEA, Evaluation Guide for the Evaluated Spent Nuclear Fuel Assay Database (SFCOMPO) NEA/NSC/R, 2015). This benchmark was studied rigorously in (Dimitri Alexandre Rochman, 2023) and can serve as a good independent reference for the impact of nuclear data uncertainties for PWRs. In particular, the issue of nuclear data uncertainties is decoupled from other uncertainties in this study.

Based on covariance data for the eight relevant main nuclides:

U-235, U-238, Pu-239, Pu-240, Pu-241, Pu-242, Am-243 and Cm-244.

600 random files were prepared, by using the SANDY code (Fiorito et al., 2017), for multiple PWR fuel element calculations. In Table 1, the uncertainty of a specific nuclide concentration from each original one, is introduced for a burnup level beyond 30 MWd/kg.

Table 2 shows that uncertainties of nuclear data in a representative

Table 1
Comparison between the cm-244 and cs-137 inventory within the cladding, obtained by the five calculation approaches. (sets 2, 3 are with 750 ppm and sets 1,4,5 with 1500 ppm boron concentration).

code	Cm-244 (Bq/g)	Cs-137 (Bq/g)
set 1	5,623E + 03	3,509E + 04
set 2	6,955E + 03	3,682E + 04
set 3	2,967E + 03	2,719E + 04
set 4	4,300E + 03	3,071E + 04
set 5	5,785E + 03	3,684E + 04

Table 2
Relative uncertainty of the ratio between the cumulative result of 600 random files and the reference case for several isotopic concentrations for the Takahama-3 samples.

isotope	Mass within a rod in FE (g)	relative uncertainty
Cm-244	5.355E-05	14 %
Pu-239	2.693E-02	1.3 %
Pu-241	5.418E-03	2.6 %
U-235	7.278E-02	5.6 %
U-238	4.384E-00	1.48 %
Sb-125	3.016E-05	0.26 %

PWR fuel rod are smaller than the differences that are observed in the fuel traces within the cladding in the current study. Thereafter, for the investigation within the cladding one has to look at other effects than nuclear data uncertainties to explore the differences. In particular, a difference between the average value and other results for Cm-244 are as high as 50 % in extreme cases. Indeed, a more extensive analysis of Table 1 reveals that set 2 overestimates Cm-244 in an unexplained manner compared to other codes. In addition, it turned out that the boron concentrations were doubled for sets 1, 4 and 5. For those cases the calculation was repeated for constant 750 ppm boron (no boron depletion) which suits better the boron concentration in set 3.

In view of the above and by excluding data set 2 the modified results are given in Table 3.:

From Table 3. it is seen that the maximum deviation from the average value for the Cm-244 inventory is reduced from 40 % to 21 %. For Cs-137, the maximum deviation from the average values stays at about 14 %. Those results emphasize the significant sensitivity of Cm-244 to the neutron fluence and the chain production elements of Cm-244. In particular, the uncertainty propagation was confirmed by analysing separately the nuclear data uncertainties of Pu-242 and Am-243, within the production chain of Cm-244. It was shown that those two isotopes increase by absolute value 5 % (out of the 14 %) the uncertainties (Table 2) for Cm-244, which means that they relative impact to other actinides is about 36 % on Cm −244 build-up.

In that sense one can explain the reason of excluding set 2 for comparing the most sensitive part of the study namely, the Cm244 comparison for such low values. As was mentioned above the expected differences between the codes could be explained by the different methods, different libraries and the basic covariance data of relevant actinides. As an example, the Jeff 3.1.2 used with the serpent code were replaced by JEFF 3.2 data which improved the converges to other codes for Cm244 by about 5 %.

However as seen in Table 1 the differences of set 2 could not be explained by all the indicators that were mentioned above and were part of this study. Nevertheless, an additional effort was performed to try to locate the roots of the discrepancies of set 2. For this purpose, the particular input of set 2 was isolated from its burnup code, cross section library and inserted in the MCNP-CINDER version. By doing so only the impact of the different geometry and cell configurations was emphasized. Strictly speaking set −2 used very detailed geometry of the full rod and many smaller cells. This could call for very fundamentals problems by Monte Carlo calculations such as statistic instabilities as well as clustering effects (Congrove et al., March 2020). A direct analysis of those geometric effects as far as the chain reaction isotope concentrations of pro Cm244 nuclides is concerned, showed indeed numerical instabilities which should be further investigated, albeit beyond the scope of this study.

The small impact on the concentration of Sb-125 emphasizes that Sb-125 is sensitive to a lesser extent to the fission process and thus to the uncertainties of the above 8 nuclides. Indeed, it was shown in a dedicated study that the Sb-125 is being produced almost completely from activation of Sn-124 and the subsequent decay of Sn-125 into Sb-125.

Altogether, the theoretical part of this study shows that an overall analysis can be done for all nuclides of interest and for extreme cases, the maximal direct deviations of nuclides' concentrations between codes is up to 25 % with the exceptional high discrepancy of Cm-244. For this extreme case, the burn up simulation methodologies on one side, and the boron concentration on the other, both have a non-negligible impact, through flux fluctuations.

From the Cs-137 results shown in Table 3., one can deduce that the fission processes within the cladding differ by 15 %. This value was confirmed also for Nd-148, which is regarded as an optimal burn up indicator.

The absorption of neutrons in U-238 in the sample serves as an indicator for the flux. Thereafter, the relation between the U-238 mass at the end and beginning of irradiation was compared between the codes and found to be 3.7 up to 4.1 %. In this regard, the above-mentioned fission indicators, Nd-148 and Cs-137, were compared additionally within the fuel pellet of the sample. In accordance with the U-238, the deviations in these burnup indicators within the fuel were also about 4 %. Consequently, the relative larger deviations seen in the cladding can be explained by the large sensitivity to the flux and reaction rate fluctuations. Strictly speaking, the different fission numbers at the cladding itself, as seen by the Nd-148 and Cs-137 contents within the cladding, results most probably from numerical and statistical factors due to the small concentration of uranium traces within the cladding, based on the fact that those differences are by far smaller within the fuel pellets. In accordance, the build-up of actinides is also proportionally affected by those effects. The general discrepancies between the simulating codes grow up from Pu-239 through Pu-242, Am-243 up to Cm-244in which the deviations are the largest due to multiple absorption reactions, each of which are affected by an uncertainty due to the number of histories within the Monte Carlo methods. In the case of deterministic codes, such deviations are "hidden" further in the solution techniques, group structures and correction factors (shielding etc.). Such analysis is more complicated and is beyond the scope of this study.

Table 3
Comparison between the calculated Cm-244 and Cs-137 inventory within the cladding, obtained by four codes with 750 ppm Boron concentration.

code	Cm-244(Bq/g)	Cs-137 (Bq/g)
set 1	5,279E + 03	3,249E + 04
set 2		
Set3	2,967E + 03	2,719E + 04
set 4	4,080E + 03	3,029E + 04
set 5	5,354E + 03	3,577E + 04

4. Experimental facility and measurement techniques

The experimental method to measure the nuclide concentrations is described in this section, upon which the experimental and simulated results are compared to get an estimation of the accuracy of the calculations and to see whether there are further effects which should be taken into account, like migration of nuclides, quality of manufacturing of the rods etc.

4.1. Fuel rod specimens

Table 4 gives an overview on fuel, cladding and irradiation data. The examined UO_2 fuel rod segment SBS1108 N0204 was initially enriched with 3.8 % U-235 and manufactured by the NIKUSI process, which is a fast oxidative, short-term sintering process at temperatures below conventional fuel fabrication procedures (Assmann et al., 1986; Kutty et al., 2004). It was irradiated in four consecutive cycles for 1226 effective full power days in the pressurised water reactor (PWR) Goesgen (KKG), Switzerland, and achieved an average burn-up of 50.4 MWd/kg as well as an average linear power of 260 W/cm upon discharge in May 1989 (Kernkraftwerk Gösgen-Däniken, 2015; B. Kienzler, V. Metz, L. Duro, A. Valls, 1st Annual Workshop Proceedings of the Collaborative Project "Fast/Instant Release of Safety Relevant Radionuclides from Spent Nuclear Fuel"(7th EC FP CP FIRST-Nuclides), 2014). During irradiation, the fuel rod segment was localised in central position within the 15 × 15 fuel assembly lattice of KKG.

4.2. Preparation and digestion process of the cladding specimens

The irradiated plenum section of fuel rod segment N0204 in the hot cells of KIT-INE is shown in Fig. 5. From the cladding segment, subsamples were cut using a low-speed saw (IsoMet 11–1180, Buehler Ltd.) equipped with a diamond wavering blade. The cutting process was performed at moderate speed in order to prevent further alteration and

Table 4
Fuel, cladding and irradiation data of the fuel rod segment SBS 1108 N0204. Data published by Kienzler et al. (B. Kienzler, V. Metz, L. Duro, A. Valls, 1st Annual Workshop Proceedings of the Collaborative Project "Fast/Instant Release of Safety Relevant Radionuclides from Spent Nuclear Fuel"(7th EC FP CP FIRST-Nuclides), 2014).

Reactor	PWR Gösgen, Switzerland
Fuel data	UO_2 fuel with 3.8 % U-235 Pellet length = 11.0 mm Pellet radius = 9.2 mm Initial O/U ratio = 2.002 Density = 10.41 g/cm^3
Cladding data	Cladding: Zircaloy-4 Cladding thickness: 0.725 mm Fuel rod diameter: 10.75 mm Initial radial gap: 0.17 mm Internal He pressure: 21.5 cm^3
Irradiation data	Average burn-up: 50.4 MWd/kg Number of cycles: 4 Average linear power: 260 W/cm Maximum linear power: 340 W/cm Date of discharge: 27.05.1989 Full power days: 1226 days Cooling time: approx. 33 years Fission gas release[a]: 8.3 %

[a] Fission gas release determined by puncturing test after 24 years of storage. Previously published by González-Robles et al. (González-Robles et al., 2016).

Fig. 5. Irradiated plenum section of fuel rod segment N0204.

heating of the sample.

The obtained Zircaloy-4 specimens were digested in a mixture of 3 % HF and 16 % H_2SO_4, which dissolved the cladding segments readily within 30 min accompanied by the production of H_2. After digestion, a thin layer of undissolved ZrO_2 was left as shown in Fig. 6.

The moderate dose rate of approximately 300 μSv/h, allowed for performing the digestion of the cladding specimens outside of the hot cell.

4.3. Analytical methods

Various analytical methods were used to analyse the different radionuclides in the digestion liquors.

Uranium as well as the transuranic isotopes, e.g., U-235,U-238, Np-237, Pu-239, Pu-240 and Pu-242, were quantified by use of an inductively coupled plasma mass spectrometer (ELEMENT XR ICP-MS, Thermo Scientific and NexION 2000, PerkinElmer), equipped with a secondary electron multiplier coupled with a Faraday detector. The respective digestion liquors were diluted to a total volume of 5 mL with

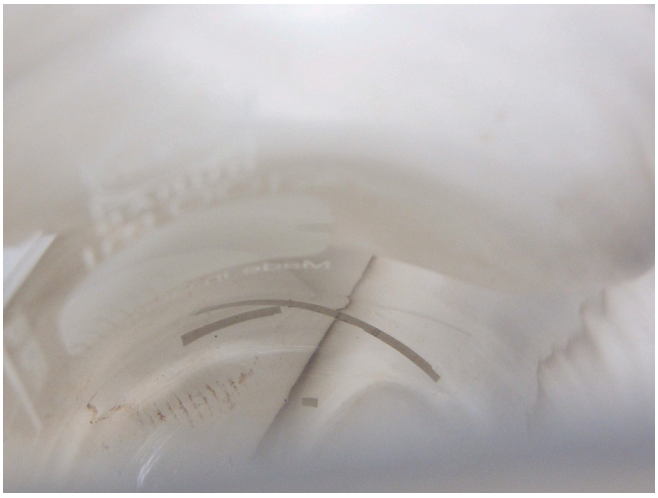

Fig. 6. Residual ZrO_2 layer after acidic digestion of the cladding specimen.

2 % HNO_3 with ranging dilution factors in order to reduce the background electrolyte concentration and to obtain the ideal concentration in the range of 1 – 10 ppb.

γ-spectrometry was utilised in order to quantify the different radionuclides according to their characteristic γ-rays, e.g., Co-60, Cs-137, and Sb-125. The measurements were performed using an extended range coaxial Ge-detector (GX3018, Canberra Industries Inc.) with an efficiency of ≥ 30 %. Energy and efficiency calibration of the detector were carried out by use of a certified multi-nuclide standard (Mixed Gamma 7600, Eckert & Ziegler Nuclitec GmbH) and data was evaluated using the Genie 2000 software (Canberra Industries Inc.).

Furthermore, activation products C-14 and Fe-55 were determined after chemical separation from the digestion liquors by liquid scintillation counting (LSC) using an ultra-low-level spectrometer (Quantulus 1220, Wallac Oy, PerkinElmer). Separation of C-14 was carried out by means of a gas extraction system, described in (Herm, 2015), whilst Fe-55 was isolated using an extraction column (Grahek and Rozmaric Macefat, 2006). From the obtained solutions aliquots of up to 3 mL were mixed with a scintillation cocktail (Hionic Fluor or Ultima Gold LLT. PerkinElmer) and the radionuclides were quantified by LSC with measuring times of 3x30 min. The uncertainties of the applied analytical methods are within a range of 5 – 10 %.

5. Comparison between measurement and simulation of the sample's plenum-cladding

A comparison of the measured and simulated data is shown in Fig. 7. The relative differences are up to 2 orders of magnitude, due to the fact that the absolute reference traces within the cladding are negligible small (3.5 ppm (Hakkinen, 2024). Additionally, the pressing of the fuel pellets into the cladding by the so called "vibrofilling" (Stratton et al., 1991) process, which causes the precipitation of fuel traces on the inner surface is of stochastically nature. As there were no other samples, it is probable that at this specific tested zircaloy ring around the plenum that more fuel dust, albeit to a negligible extent, has precipitated on the cladding. Evidently, this leads to relative higher concentration of actinides and fission products in comparison with the simulations.

Nevertheless, those negligible amounts of actinides were to a satisfactory extent calculated by different codes as shown above. Strictly speaking, the absolute measured amount is still very low as far as radiation damage is concerned, about 4–5 order of magnitudes smaller than the expected dose from the fuel itself. On the other side, the ability to measure and calculate, those fuel traces at very high accuracy, increases the reliability of the postulated cladding integrity at the repository site.

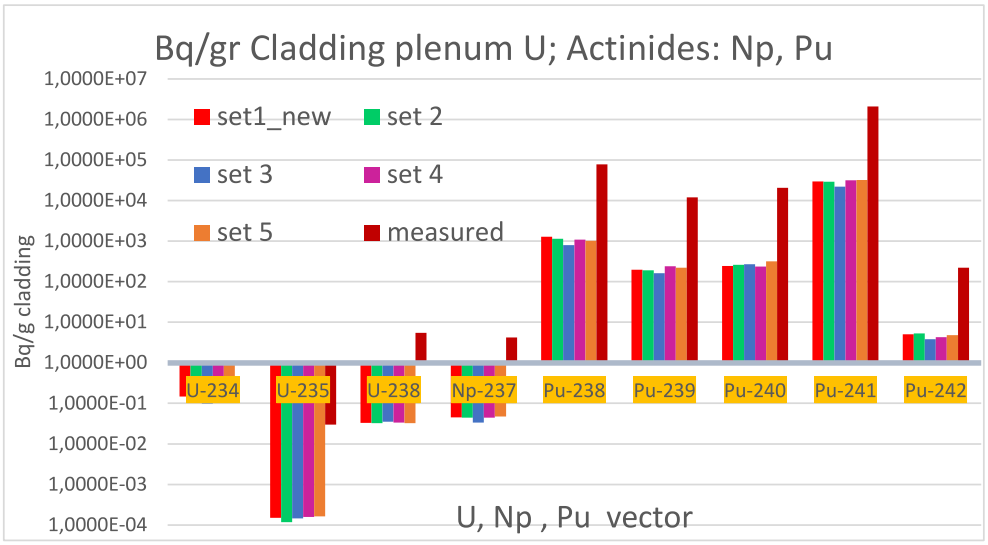

Fig. 7. Comparison of the calculated and measured inventory of uranium, neptunium and plutonium isotopes. The large differences imply clearly of fuel adherence to the cladding, most probably during the fuel rod preparation and operation.

The measured concentration of Cs-137 is another special case. The larger concentration ratio in Fig. 8 is corollary to the migration of gaseous Cs-137 from the pellets to the plenum and its precipitation on the inner side of the cladding. This migration for gaseous elements is stronger within the pellets by temperature over 1000 °C based on the evaporation temperature at 641 °C and by lower temperature in the plenum it retains on the inner surface of the cladding.

The measurement of C-14 concentrations concerns the long-term biological hazards due to its beta decay with 5730 years half-life. C-14 is mainly produced by neutron reaction with N-14 and to lesser extent by O-17 and C-13. Thereafter, for the measurement serves as an indicator of the initial nitrogen content in the Zry-4 cladding. This latter idea of using measurements for re-evaluation of the original composition of specific elements can be extended also to cobalt and tin. Based on the relatively good results of all codes concerning Co-60 and Sb-125, one can estimate, in a similar manner as for N-14, the amount of the Co-59 and Sn-124 concentrations respectively. One should mention that the contribution of iron and nickel is by far lower (factor 500) as far as the production of Co-60 is concerned. Nevertheless, some iron isotopes can be estimated. For example, the enhanced measured Fe-55 value indicates generally on the initial Fe-54 content. However, in this study one should be aware that the cladding in the plenum was in touch with the spring within it, so like in the case of the fuel traces, discussed above, the measured results of the iron were affected by traces coming from the steel spring in the plenum. Consequently, a clear quantitative estimation of the iron content is not possible in this study in the manner that it is done for N-14, Co-59 and Sn-124.

6. Conclusions

This paper presented the results and analyses of various calculation approaches to calculate the radionuclide inventory in irradiated cladding samples, resulting from activation of cladding base material and impurities. A code-to-code verification is performed. Then, a

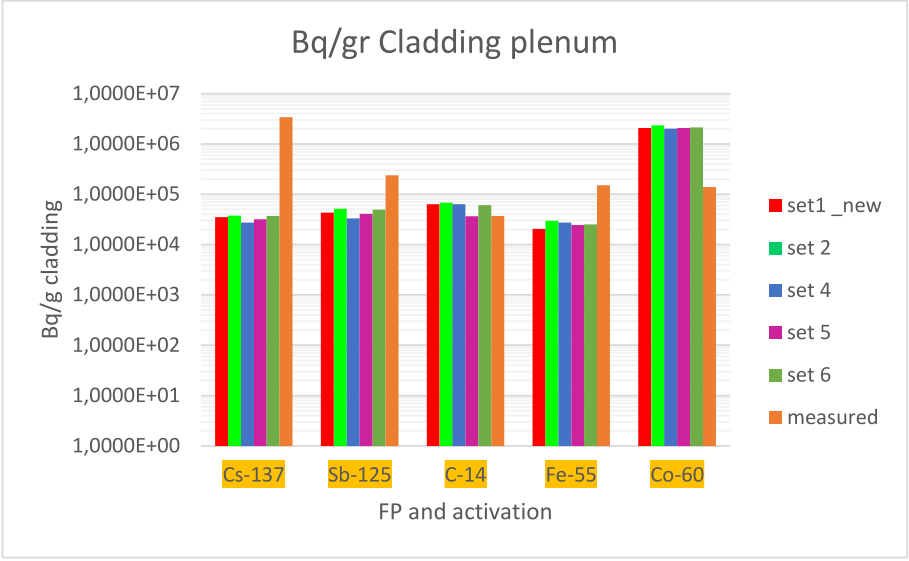

Fig. 8. Comparison of the calculated and measured inventory of Cs-137 and other activation products. The large amount of Cs-137 indicates material migration from the fuel to the cladding as function of the evaporation temperature. The reduced amount of Co-60 is mostly due to the enhanced estimated amount of Co-59 within the cladding, by about factor 10. The differences by Sb-125 could be explained by the simulated concentration of Sn-124.

comparison between all calculations and measurements conducted by the KIT at the INE facilities is presented. Overall consistency between the calculations is observed. Small differences were attributed to using different methods, such as stochastic vs deterministic methods, nuclear data, and different depletion modules. Most important, the consistency between the various methods is considered sufficient for the practical purposes of the relevant applications.

The usage of this new and reliable measurement technique, allowing accurate and precise evaluation of the radionuclides in the analysed samples is demonstrated. Comparing the calculated to measured C-14, the consistency between the calculated C-14 and the measured values is already promising, being a relevant radionuclide for the long-term disposal of SNF that is produced almost entirely through activation of impurities in the cladding. In addition, the ability of estimating the initial contents of elements in the cladding as shown for Co-59 and Sn-124 is quite promising.

Differences between all the calculations and the measured values of the actinides and the fission products indicate the potential presence or migration of fuel traces in the cladding samples (including actinides, fission products, and possibly other nuclides). The most probable reason for those differences is the stochastic nature of the ‘‘vibrofilling’’ manufacturing technique, and contact between the fuel and cladding in fabrication and operation. In any case, the additional amount of traces is by far negligible compared to the actinides produced in the fuel. It is only due to the high purity of the cladding with only about 3.5 ppm of uranium, that the relative differences to the calculations are by up to 2 orders of magnitude.

Further investigations are required to analyse the extent of different mechanisms attributing to the radionuclides reaching the cladding samples and the parameters influencing these processes.

From a theoretical point of view, the differences between the codes, which were performed on realistic conditions, and available input, illuminate the need of improvement and analysis of the simulation tools. In particular, the nuclide chain of building Cm-244 is very sensitive to the flux fluctuations and to the stochastic nature of the solutions. In parallel, further research should concentrate on the effect of energy group based deterministic codes, the burn up module, the handling of simulated number of shutdown days between each step and the nuclear data libraries.

Declaration of competing interest

The authors declare that they have no known competing financial interests or personal relationships that could have appeared to influence the work reported in this paper.

Acknowledgement

This document is a report of the European Joint Programme on Radioactive Waste Management (EURAD). EURAD has received funding from the European Union’s Horizon 2020 research and innovation programme under grant agreement No 847593.

Data availability

The data that has been used is confidential.

References

A. Shama et al. “Validation of spent nuclear fuel decay heat calculations using Polaris, ORIGEN and CASMO5”. In: Annals of Nuclear Energy 165 (2022), p. 108758. issn: 0306-4549. doi: https://doi.org/10.1016/j. anucene.2021.108758. url: https://www.sciencedirect.com/science/article/pii/S0306454921006344.

A. Alraisi, Y. Yi., S. Lee, S. A. Alameri, M. Qasem, C. Y. Paik , “Effects of ATF cladding properties on PWR responses to an SBO accident, A sensitivity analysis”, Annals of nuclear energy ANE Vol 165, 2022.

Alvarez-Velarde, F., Gonzalez-Romero, E.M., Rodrıguez, I.M., 2014. Validation of the burn-up code EVOLCODE 2.0 with PWR experimental data and with a Sensitivity/Uncertainty analysis. Ann. Nucl. Energy 73, 175–188. https://doi.org/10.1016/j.anucene.2014.06.049.

Assmann, H., Dörr, W., Peehs, M., 1986. Control of UO2 Microstructure by Oxidative Sintering. J. Nucl. Mater. 140, 1–6. https://doi.org/10.1016/0022-3115(86)90189-3.

B. Kienzler, V. Metz, L. Duro, A. Valls, 1st Annual Workshop Proceedings of the Collaborative Project “Fast/Instant Release of Safety Relevant Radionuclides from Spent Nuclear Fuel”(7th EC FP CP FIRST-Nuclides), 2014.

B.J. Ade. SCALE/TRITON Primer: A Primer for Light Water Reactor Lattice Physics Calculations. Tech. rep. ORNL/TM-2011/21 and NUREG/CR-7041. Oak Ridge National Laboratory, USA, Nov. 2012.

Congrove, P., Schwageraus, E., Parks, G.T., March 2020. Neutron clustering as a driver of Monte Carlo burn-up instability. Annals of Nuclear Energy 137.

Dimitri Alexandre Rochman, 2023. Francisco´ Alvarez-Velarde, Ron Dagan, Luca Fiorito, Silja H¨akkinen, Marjan Kromar, Ana Mu¯noz, Sonia Panizo-Prieto, Pablo Romojaro, Peter Schillebeeckx, Marcus Seidli, Ahmed Shama, and Gasper Zerovnik “On the estimation of nuclide inventory and decay heat: a review from the EURAD European project” EPJ Nuclear Science. Technology 9.

P. Doyle, J. Stuckert, M. Grosse, M. steinbrueck, A. T. Nelson, J. HArp, K. TerranAnalysis of iron-chromium-aluminum samples exposed to accident conditions followed by quench in the QUENCH-19 Experiment”, Journal of Nuclear materials, Vol 580, 2023.

Fiorito, L., ˙Zerovnik, G., Stankovskiy, A., Van den Eynde, G., Labeau., P., 2017. Nuclear data uncertainty propagation to integral responses using SANDY. Annals of Nuclear Energy 101, 359–366.

F. Gallmeier, E. Iverson, W. Ferguson, J. S. T. HOLLOWAY, CH. KELSEY, G. MUHRER, ICANS XIX, B. MICKLICH, M. WOHLMUTHER, “THE CINDER’90 TRANSMUTATION CODE PACKAGE FOR USE IN ACCELERATOR APPLICATIONS IN COMBINATION WITH MCNPX” 19th Meeting on Collaboration of Advanced Neutron Sources March 8 - 12, 2010, Grindelwald, Switzerland.

González-Robles, E., Metz, V., Wegen, D.H., Herm, M., Papaioannou, D., Bohnert, E., Gretter, R., Müller, N., Nasyrow, R., de Weerd, W., Wiss, T., Kienzler, B., 2016. Determination of fission gas release of spent nuclear fuel in puncturing test and in leaching experiments under anoxic conditions. J. Nucl. Mater. 479, 67–75. https://doi.org/10.1016/j.jnucmat.2016.06.035.

Grahek, Z., Rozmaric Macefat, M., 2006. Extraction chromatographic separation of iron from complex liquid samples and the determination of 55Fe. J. Radioanal. Nucl. Chem. 267, 131–137.

S. Häkkinen „Impurities in LWR fuel and structural materials” VTT-R-00184-20 VTT.

Herm, M., 2015. Study on the effect of speciation on radionuclide mobilization - C-14 speciation in irradiated Zircaloy-4 cladding and nitrate / chloride interaction with An(III) / Ln(III). Karlsruhe Institute of Technology.

Kernkraftwerk Gösgen-Däniken, A.G., 2015. Technik Und Betrieb - Technische Hauptdaten.

C. Kim, C. Tong, M. Grosse, Y. Moeng, C.Jang, M. steinbrueck, „Oxidation mechanism and kinetics of nuclear-grade FeCrAl alloys in the temperature range of 500–1500 °C in steam”, Journal of Nuclear Materials, Vol. 564, 2022. https://doi.org/10.1016/j.jnucmat.2022.153696.

Kutty, T.R.G., Hegde, P.V., Khan, K.B., Jarvis, T., Sengupta, A.K., Majumdar, S., Kamath, H.S., 2004. Characterization and densification studies on ThO2-UO2 pellets derived from ThO2 and U3O8 powders. J. Nucl. Mater. 335, 462–470. https://doi.org/10.1016/j.jnucmat.2004.08.003.

Leppänen, et al., 2015. The Serpent Monte Carlo code: Status, development and applications in 2013. Annals of Nuclear Energy 82, 142–150. https://doi.org/10.1016/j.anucene.2014.08.024.

Michel-sendis, F., Gauld, I., Martinez, J.S., Alejano, C., Bossant, M., Boulanger, D., Cabellos, O., et al., 2017. SFCOMPO-2.0: An OECD NEA database of spent nuclear fuel isotopic assays, reactor design specifications, and operating data. Annals of Nuclear Energy ANE 110, 779–788.

OECD NEA, Evaluation Guide for the Evaluated Spent Nuclear Fuel Assay Database (SFCOMPO) NEA/NSC/R(2015) 8, February 2016. www.oecd-nea.org/sfcompo.

ORIGEN2.2 ORNL, USA, CCC-371, 2002.

M. Pusa and J. Leppänen. “Computing the Matrix Exponential in Burnup Calculations”. In: Nuclear Science and Engineering 164.2 (2010), pp. 140–150. doi: 10.13182/NSE09-14. eprint: https://doi.org/10.13182/NSE09- 14. url: https://doi.org/10.13182/NSE09-14.

B. Qiu, J. Wang, Y. Deng. M. Wang, Y. WuS. Z. Qiu, „A review on thermohydraulic and mechanical-physical properties of SiC, FeCrAl and Ti3SiC2 for ATF cladding”, Nuclear Engineering and Technology, Vol 52 , issue 1 2020.

Sjöland et al, “Spent nuclear fuel management, characterisation, and dissolution behaviour: progress and achievement from SFC and DisCo” NPJ N, https://doi.org/10.1051/epjn/2022029, 2023.

M. Steinbrueck , M. Grosse, C. Tang, Juri Stuckert, H. Juergen Seifert, “An Overview of Mechanisms of the Degradation of Promising ATF Cladding Materials During Oxidation at High Temperatures”, https://doi.org/10.1007/s11085-024-10229-y, 2024, Springer publishing.

W.R. Stratton, F. Botta, R. Hofer, G. Ledergerber, F. Ingold, C. Ott, J. Reindl, H.U. Zwicky, R. Bodmer, F. Schlemmer, A comparative irradiation test of UO2 sphere-pac and pellet fuel in the Goesgen PWR., in: Int. Top. Meet. LWR Fuel Perform. “Fuel 90’s,” Avignon, France, 1991: pp. 174–183.

-Žerovnik, G., Ambrožič, K., Čalič, D., Fiorito, L., Govers, K., Hernandez Solis, A., Kos, B., Kromar, M., Schillebeeckx, P., Stankovskiy, A.: Characterisation of spent PWR fuel for decay heat, neutron and gamma-ray emission rate: code comparison,’ Proceedings of the International Conference on Mathematics and Computational Methods applied to Nuclear Science and Engineering (M&C 2019), Portland, USA, 25. – 29. August 2019, pp. 2736-2745.